Free space quantum key distribution over 500 meters using electrically driven quantum dot single-photon sources—a proof of principle experiment

2014 New J. Phys. 16 043003

(http://iopscience.iop.org/1367-2630/16/4/043003)

New Journal of Physics
The open access journal at the forefront of physics
Deutsche Physikalische Gesellschaft DPG | IOP Institute of Physics

Free space quantum key distribution over 500 meters using electrically driven quantum dot single-photon sources—a proof of principle experiment

Markus Rau[1,6], Tobias Heindel[2,4,6], Sebastian Unsleber[2], Tristan Braun[2], Julian Fischer[2], Stefan Frick[1], Sebastian Nauerth[1], Christian Schneider[2], Gwenaelle Vest[1], Stephan Reitzenstein[2,4], Martin Kamp[2], Alfred Forchel[2], Sven Höfling[2,5] and Harald Weinfurter[1,3]

[1] Fakultät für Physik, Ludwig-Maximilians-Universität München, Germany
[2] Technische Physik and Wilhelm Conrad Röntgen Research Center for Complex Material Systems, Universität Würzburg, Germany
[3] Max-Planck-Institut für Quantenoptik, Garching, Germany
E-mail: markus.rau@physik.uni-muenchen.de

Received 18 September 2013, revised 26 February 2014
Accepted for publication 3 March 2014
Published 7 April 2014

New Journal of Physics **16** (2014) 043003
doi:10.1088/1367-2630/16/4/043003

Abstract

Highly efficient single-photon sources (SPS) can increase the secure key rate of quantum key distribution (QKD) systems compared to conventional attenuated laser systems. Here we report on a free space QKD test using an *electrically* driven quantum dot single-photon source (QD SPS) that does not require a separate laser setup for optical pumping and thus allows for a simple and compact SPS QKD system. We describe its implementation in our 500 m free space QKD system in downtown Munich. Emulating a BB84 protocol operating at a repetition rate of 125 MHz, we could achieve sifted key rates of 5–17 kHz with error ratios of 6–9% and $g^{(2)}(0)$-values of 0.39–0.76.

Keywords: QKD, quantum key distribution, quantum dots, electrically driven, free space

[4] Present address: Institut für Festkörperphysik, Technische Universität Berlin, Germany
[5] Present address: SUPA, School of Physics and Astronomy, University of St Andrews, UK
[6] These authors have contributed equally to this work.

1. Introduction

Quantum key distribution (QKD) [1] is the first commercially available method of quantum information [2]. Experimental QKD systems have reached GHz repetition rates [3–5], distances beyond 200 km [6], and have been successfully implemented in secure networks of QKD links [7, 8]. Often, strongly attenuated laser pulses are used, which means that the emitted states of light contain multiple photons with a certain probability. Since the security of QKD relies on the quantum mechanical properties of single quanta, an eavesdropper can gain information on the key without being discovered by measuring multi-photon pulses. Yet, decoy protocols allow one to efficiently put an upper bound on this information leakage [9] and enable the use of laser pulses with an intensity of $\simeq$0.5 photons, yielding a probability of 30% for a single photon in each pulse. Replacing the laser source in such a system with a single-photon source (SPS) that has a higher single-photon emission probability will increase the secret key rate. It was also shown that QKD systems using an efficient SPS can generate a key at higher channel losses than systems using attenuated laser pulses [10], or alternatively, that for a SPS with sufficiently small $g^{(2)}(0)$-value a decoy protocol is not necessary to efficiently generate a secret key [11]. Moreover, in the regime of high channel transmission, a QKD system can be limited by the receiver's single-photon detector maximum rate. In this scenario, the only possibility to increase the key rate is reducing the fraction of multi-photon states (i.e., using SPSs).

An efficient type of SPS is based on self-assembled quantum dots (QDs). So far, most experiments with QD SPSs [12–16] used an optical excitation scheme. Recently, we demonstrated that QKD is possible with electrically driven QD SPSs in a lab system [17]. This new excitation scheme significantly reduces the complexity of the optics and its costs, since no additional laser system is required. This allows for a much tighter integration into a QKD system and paves the way to practical applications.

Here we report on the evaluation of an electrically driven QD SPS implemented in the realistic environment of a free space QKD testbed in downtown Munich. With a 500 m quantum channel connecting two telescopes on the rooftops of university buildings, the QD SPS setup had to be operated in the attic, without regular lab environment. Important challenges arising during the design of the QKD system were the implementation of an optical system for the operation of the QD SPS under these adverse conditions and the implementation of a polarization modulator at 125 MHz in the outdoor telescope.

2. QKD System

2.1. Quantum dot single-photon source

The single-photon source used in this experiment consists of a single layer of self-organized InAs QDs embedded in an intrinsic λ-cavity sandwiched between an n-doped and a p-doped distributed Bragg reflector (DBR). A cross-sectional scanning electron microscopy (SEM) image of a fully processed device is displayed in the left panel of figure 1(a). The micropillar structure (diameter 2.0 μm) with a moderate Q-factor (1300) enables a high overall efficiency, (i.e., the probability to obtain one photon in the output mode of the resonator per electrical excitation pulse). A source created in the same manufacturing process as the one used here already demonstrated values of up to 34% under pulsed electrical current injection [18]. Figure 1(b) displays the micro-electroluminescence (μEL) spectrum of the QD SPS utilized in

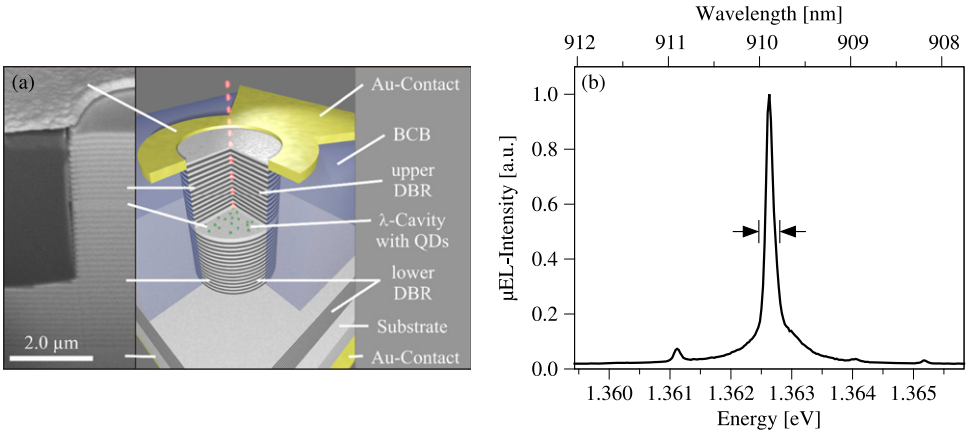

Figure 1. (a) Cross-sectional SEM image (left) and schematic (right) of an electrically contacted quantum dot single-photon source (QD SPS). (b) Micro-electroluminescence (μEL) spectrum of the QD SPS triggered at 125 MHz ($T = 56$ K, pulse height 4.75 V, pulse width 1 ns, bias voltage 2.0 V). Arrows indicate the width of the bandpass filter ($\Delta\lambda = 0.23$ nm) used during the experiment.

the QKD experiment operated at a repetition rate of 125 MHz, where spectral resonance of a single QD emission line with the fundamental cavity mode of the resonator was achieved via temperature tuning at $T_{res} = 56$ K.

The optical setup for the SPS was situated in an attic room from where light was guided to the rooftop via a single mode fiber. Using a QD SPS for QKD foremost requires highly efficient coupling of the emission to the remaining setup. Furthermore, at this proof of principle level the ability for a spectral characterization and a measurement of the $g^{(2)}(0)$-value is quite useful at the location. While such a setup can easily fill the better part of a lab, the room for our setup was very restricted, and effectively only allowed for the accommodation of a breadboard (75 cm × 120 cm) for the source and a standard 19-inch server rack. Moreover, the room was not providing a standard lab environment such as air conditioning, etc.

Since transporting liquid helium to the setup was not feasible, a closed-cycle pulse tube cryostat was used (Cryomech PT403), which allowed for cooling the QD SPS down to 20 K. The pulse tube was mounted separately from the valve unit to avoid vibrations from moving mechanical parts. To minimize the effect of any remaining vibrations, the microscope objective (NA 0.68) used to collect the source's emission was mounted on the cryostats cold finger. We observed a movement of the source's position with an amplitude of about 0.5 μm at the pulse tube's pumping frequency (1 Hz), but as the lens was fixed relative to the QD the count rates observed later were not affected by this. The sample was excited by an electrical pulse generator providing pulses with widths down to 200 ps (full-width at half-maximum) and repetition rates of up to 250 MHz via radio frequency vacuum feedthrough. In addition, a DC-offset could be applied to the sample.

Outside the cryostat, the QD SPS emission was spectrally selected by angle-tuning a narrow interference bandpass filter (Andover Corporation $\lambda_{max} = 910$ nm, $T = 48\%$, $FWHM = 0.23$ nm) (cf figure 1(b)). After spectral filtering, the emission was coupled into a 20 m long single-mode fiber to guide it to the telescope system on the rooftop. A multi-mode fiber could have reduced the coupling losses here; however, a single-mode beam is required in

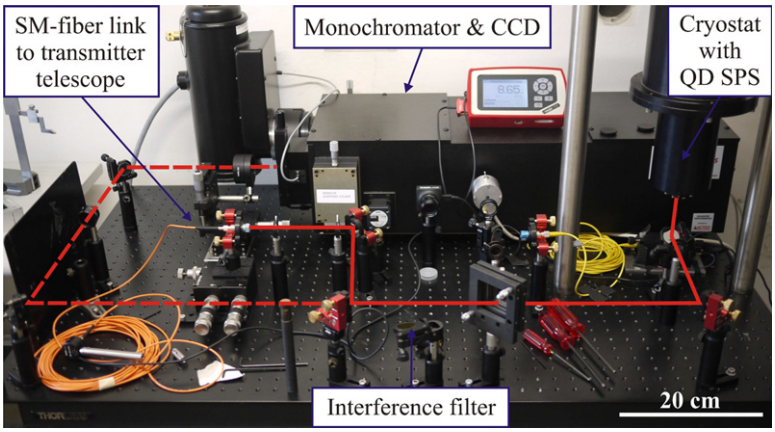

Figure 2. Picture of the module hosting the quantum dot single-photon source (QD SPS) used for the quantum key distribution experiment: The breadboard includes a closed-cycle cryostat, a monochromator with an attached charged coupled device (CCD) camera, an interference bandpass filter, and the single-mode (SM-) fiber link to the transmitter telescope. The picture was taken during the initial alignment of the setup, when a multi-mode fiber was attached to the fiber link port.

connection with the electro-optical modulator and to efficiently bridge the 500 m quantum channel link. For an evaluation of the source parameters, it was possible to connect the emission to a fiber-coupled Hanbury-Brown and Twiss (HBT) setup to measure the second order photon autocorrelation, which enabled the extraction of the actual $g^{(2)}(0)$-value, or to a monochromator to acquire the spectrum.

A picture of the optical setup is shown in figure 2. It is worth noting that the monochromator took up roughly half of the breadboard. If high-resolution spectrometry is not required in routine operation, the whole setup could be shrunk even further and then fit into a single 19-inch server rack, with some additional room for the cryostats helium compressor and an air-cooled water chiller (both $\approx 0.5^3$ m^3).

2.2. Free space optical system

The single photons from the QD SPS in the attic were guided to Alice's telescope system on the rooftop via a 20 m single-mode fiber. In Alice's telescope system, first the polarization of the pulses, which are initially unpolarized[7], was set (figure 3). For this purpose light from the single-mode fiber passed a thin film polarizer followed by a high-bandwidth electro-optical modulator (Quantum Technology TWAM, traveling-wave design, driven by high-bandwidth amplifier MODEL 3520A) to prepare the four BB84 polarization states. For the alignment of Alice's polarization directions with those of Bob's, two waveplates were used together with a change of the bias voltage in the modulator. The beam was then collimated with a 3-inch lens into the quantum channel. To allow for a precise alignment of the telescope, all optical

[7] The emission is unpolarized due to the circular cross section of the QD SPS. Slight asymmetries of the micro-resonator can lead to an energetic splitting of two orthogonal linearly polarized modes on the order of 10 μeV [19]. This is much smaller than the cavity modes' spectral width ($\approx$1 meV) and does not cause the emission to become polarized.

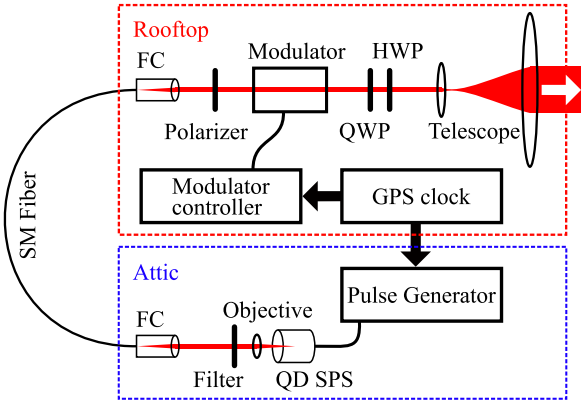

Figure 3. Scheme of the sender setup. Two fiber couplers (FC) and a 20 m single-mode (SM) fiber connect the quantum dot single-photon source (QD SPS) in the attic with the telescope system on the rooftop. The quarter and half wave plate (QWP/HWP) are used to align the polarization directions to the receivers.

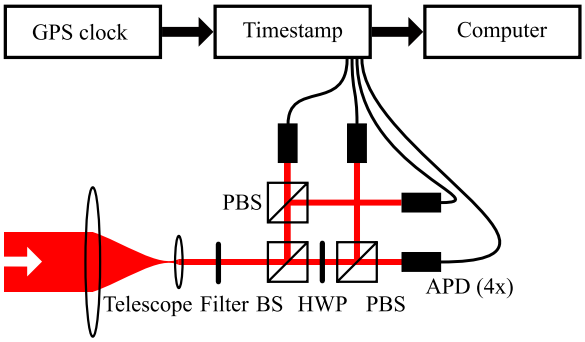

Figure 4. Scheme of the receiver setup. A nonpolarizing beamsplitter (BS) is used to randomly choose the measurement basis. The polarization analysis is done by a polarizing beamsplitter (PBS) for horizontal/vertical polarizations, and a half wave plate (HWP) together with a PBS for +45°/−45° polarizations.

components were mounted on a single breadboard movable with stepper motors. The breadboard was fitted into a rugged aluminum box to shield the components against weather. Power consumption was largely determined by the cryostats helium compressor (3.4 kW) in the attic and the high-bandwidth amplifier on the rooftop (0.5 kW).

Bob's system essentially resembles the one used previously with attenuated laser pulses (figure 4) [7]. Here a 3-inch telescope collects the light coming from the quantum channel, followed by a 40 nm wide bandpass filter, and a four-channel polarization analyzer with passive basis choice using four Si-APDs with a 500 μm diameter [20]. Similar to Alice's system, the setup is shielded by a metal box, and the whole optical system can be tip-tilted for alignment.

2.3. Electronic control

To perform a QKD protocol, an absolute temporal synchronization between Alice and Bob is necessary in order to correlate Bob's detection events with the pulses Alice sent. Instead of an additional free space optical transmission of a clock signal, which is highly susceptible to short

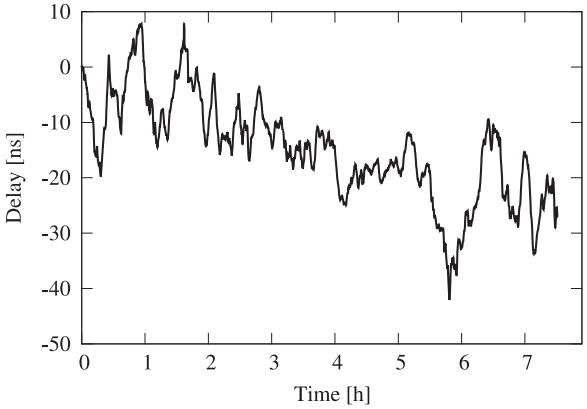

Figure 5. Delay between the two sinusoidal outputs of the two 10 MHz GPS Oscillators used in this experiment. The data was taken during a preliminary measurement with both Oscillators connected to one oscilloscope.

breaks in transmission, we used two GPS disciplined oscillators (crystal ovens tuned to the GPS time reference), one each at Alice and Bob, as a common 10 MHz frequency base. Although their long-term frequency accuracy is very high, they can drift on short time scales: the frequency stability is specified with an Allan deviation of 1×10^{-11} to 2×10^{-11} for averaging times of 1 to 100 seconds. To determine the effect on the phase stability we recorded the time delay between the 10 MHz signal of the clocks every 5 s. The result of this measurement is shown in figure 5. The drifts of several nanoseconds on typical timescales of a few minutes had to be compensated, or time filtering with narrow acceptance windows would have been impossible.

On Alice's side the GPS reference was converted to a 125 MHz clock signal used as a trigger for the source's electrical pulse generator and, with the respective delay, as a clock signal for the control system of the electro-optical modulator. The attic and rooftop stations were thus only connected with a twin coax cable for the differential clock signal and the single-mode fiber for the single photons.

To control the modulator a custom-built 16-bit arbitrary waveform generator was used to generate a programmable analog waveform, which was fed to the high-bandwidth amplifier (all components of the modulation system have a bandwidth >500 MHz). In the experiment we used a staircase-shaped waveform of four voltage levels to generate a fixed pattern of polarizations (H $\rightarrow$ +45° $\rightarrow$ V $\rightarrow$ −45°) at a rate of 125 MHz, which is sufficient to determine the sifted key rate and error ratio for this proof of principle experiment.

On Bob's side the detection events were registered by a timestamping unit (75 ps resolution) locked to Bob's GPS reference and transferred to a PC. A software compensation of the drifts of Bob's GPS oscillator relative to Alice's was performed by determining the average phase of detection events over 0.5 s and using it to update an offset relative to Bob's GPS clock signal. Then, time filtering deselected all events outside a time window[8] of variable width between 1.8 ns and 2.2 ns around the expected arrival times of Alice's pulses. After a key sifting

[8] At the higher excitation settings the SPSs pulses were slightly longer compared with lower settings, requiring a longer time window.

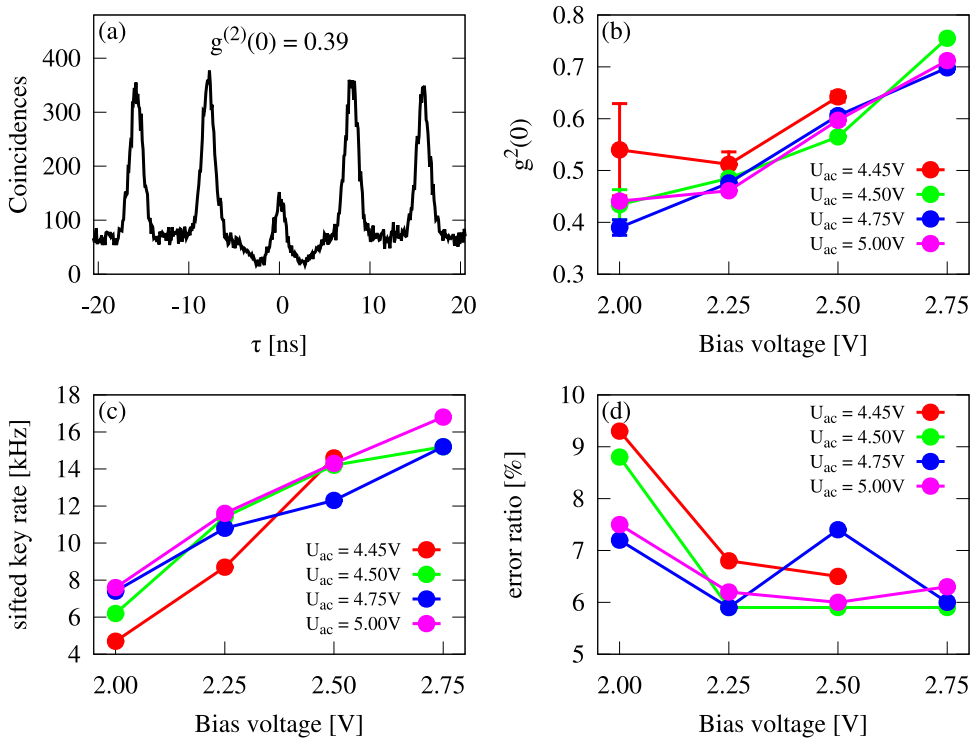

Figure 6. (a) Photon autocorrelation measurement (216 second integration time, 163.6 kHz total detection rate in both APDs) of the single-photon source's pulsed emission (f_{rep} = 125 MHz, pulse height 4.75 V, bias voltage 2.00 V). (b)–(c) $g^{(2)}(0)$ value, sifted key rate and error ratio measured at different values of the bias voltage and the height U_{AC} of the electrical pulses driving the source. All error bars in (c) and (d) are inside the points.

step, the error ratio was determined by comparing the events with the known pattern of polarizations.

3. Experiment

As a first step, the initial alignment of the telescopes' orientations and of polarization directions was achieved using a bright guiding laser coupled into Alice's SM-fiber, followed by coupling the pulses from the QD SPS. The SPS operated at a repetition rate of 125 MHz and a temperature of T_{res} = 56 K. We used a series of parameter settings for the offset and height of the electrical pulses driving the QD, starting with an offset of 2.00 V and a height of 4.45 V and ending with 2.75 V offset and 5.00 V height. The pulse width was set to 1 ns for all measurements. At each setting the $g^{(2)}(0)$-value was determined by an autocorrelation measurement with an integration time between 1 and 22.5 minutes, and the sifted key rate and error ratio were measured and averaged for 100 seconds.

The autocorrelation measurements showed that the $g^{(2)}(0)$-value varied between 0.39 to 0.76 (figures 6(a) and (b))[9]. With raising bias voltage we observed on average an increase of the source's emission rate due to an increase of the carrier capture rate into the QD. This is

accompanied by an increase of $g^{(2)}(0)$ due to the increasing contribution of uncorrelated background emission feeding the optical mode. At the highest setting, the pulses from the QD SPS had an average photon number of $\mu_{SPS} = 0.084$[10], but losses inside Alice's system including the objective (T = 70%), cryostat window (97%), interference filter (48%), coupling into the single-mode fiber (38%), the polarizer (50%), eight mirrors (82%), and the modulator (80%), reduced the overall intensity of the pulses from Alice's system to $\mu_{Alice} = 0.0034$.

On Bob's side we observed the sifted key rate increasing from 5 to 17 kbit s^{-1} (figure 6(c)) as the intensity of the pulses increased with the bias voltage applied to the SPS. From the detection rates and the value of μ_{Alice} we calculated that the attenuation of the quantum channel from the exit of Alice's telescope to a detection in Bob's module was 10 dB. This number includes all losses along the free space transmission or in Bob's optical components, and the inefficiency of the single-photon detectors.

The error ratio decreased from 9% at the lowest excitation setting to 6% at the highest settings (figure 6(d)), of which 4% can be attributed to the contrast ratio of the modulator (1:25) and the remaining 2% to background events during the detection time windows. Performing experiments at night, each of the four detectors registered a background count rate of 1 kHz, caused by roughly equal amounts of dark counts and events from ambient light, resulting in a total background count rate of 4 kHz. Due to the time filtering with an acceptance window of 1.8 ns–2.2 ns (varying with the electric pulse offset), about 25% of the background events contributed to the sifted key.

We conclude that the high losses inside Alice's system should be reduced by a tighter integration of the source with a polarization modulator without a connecting fiber or other interjacent components. Using single-photon detectors, which are more optimized for the QDs emission wavelength, and current advances in device manufacturing like polarized and positioned quantum dots [21–25] will allow increase in the overall performance of QKD systems using QD SPSs significantly.

4. Summary

We successfully demonstrated the feasibility of QKD using electrically pumped QD SPSs on a 500 m free space link connecting two buildings in downtown Munich. This proves that this type of source can be used in a practical deployment scenario for a QKD system. If used in a BB84 protocol, our demonstration setup would yield sifted key rates between 5 and 17 kHz, with $g^{(2)}(0)$-values from 0.39 to 0.76 (figure 6). Although about two orders of magnitude increase in efficiency are required to be competitive with attenuated pulse systems, we could show that

[9] $g^{(2)}(0)$-values were extracted from the raw data by integrating the zero-delay peak over one full pulse period and dividing the result by the average area of the remaining peaks. Compared to our previous work [17] the reduced single-photon purity is mainly due to a higher spectral density of QD emission lines in spectral vicinity of the resonator mode and due to the higher resonance temperature of this particular device, both of which lead to enhanced uncorrelated background emission from the fundamental optical mode.

[10] The value for μ_{SPS} is determined from the count rate observed during the autocorrelation measurement, by taking the losses mentioned in the text into account and assuming an APD quantum efficiency of $\eta = 0.35$. The somewhat lower overall efficiency of the SPS if compared to the values reported in [18] is attributed to a spatial mismatch of the emitter with respect to the cavity mode and the higher operating temperature of the present device.

electrically driven QD SPSs can be operated outside a lab environment with minimal space requirements. Further improvements in the fabrication of the QD SPSs together with a better coupling of the single-photon emission into the quantum channel will enable one to perform efficient QKD with electrically driven QD SPSs in a range competitive with state-of-the-art attenuated laser systems.

Acknowledgments

The authors gratefully acknowledge expert sample preparation by M Emmerling and A Wolf as well as financial support by the German Ministry of Education and Research through the project QPENS and QUASAR.

References

[1] Bennett C H and Brassard G 1984 Quantum cryptography: Public key distribution and coin tossing *Proc. of IEEE Int. Conf. on Computers Systems and Signal Processing* vol 175 (New York: IEEE)
[2] Moore S K 2007 Commercializing quantum keys *IEEE Spectrum* **44** 15
[3] Gordon K J, Fernandez V, Buller G S, Rech I, Cova S D and Townsend P D 2005 Quantum key distribution system clocked at 2 GHz *Opt. Express* **13** 3015
[4] Namekata N, Takesue H, Honjo T, Tokura Y and Inoue S 2011 High-rate quantum key distribution over 100 km using ultra-low-noise, 2-GHz sinusoidally gated InGaAs/InP avalanche photodiodes *Opt. Express* **19** 10632
[5] Dixon A R, Yuan Z L, Dynes J F, Sharpe A W and Shields A J 2010 Continuous operation of high bit rate quantum key distribution *Appl. Phys. Lett.* **96** 161102
[6] Liu Y *et al* 2010 Decoy-state quantum key distribution with polarized photons over 200 km *Opt. Express* **18** 8587
[7] Peev M *et al* 2009 The SECOQC quantum key distribution network in Vienna *New J. Phys.* **11** 075001
[8] Sasaki M *et al* 2011 Field test of quantum key distribution in the Tokyo QKD network *Opt. Express* **19** 10387
[9] Ma X, Qi B, Zhao Y and Lo H K 2005 Practical decoy state for quantum key distribution *Phys. Rev.* A **72** 012326
[10] Wang Q, Chen W, Xavier G, Swillo M, Zhang T, Sauge S, Tengner M, Han Z F, Guo G C and Karlsson A 2008 Experimental decoy-state quantum key distribution with a sub-poissionian heralded single-photon source *Phys. Rev. Lett.* **100** 90501
[11] Waks E, Santori C and Yamamoto Y 2002 Security aspects of quantum key distribution with sub-poisson light *Phys. Rev.* A **66** 042315
[12] Waks E, Inoue K, Santori C, Fattal D, Vuckovic J, Solomon G S and Yamamoto Y 2002 Quantum cryptography with a photon turnstile *Nature* **420** 762
[13] Aichele T, Reinaudi G and Benson O 2004 Separating cascaded photons from a single quantum dot: Demonstration of multiplexed quantum cryptography *Phys. Rev.* B **70** 235329
[14] Intallura P M, Ward M B, Karimov O Z, Yuan Z L, See P, Atkinson P, Ritchie D A and Shields A J 2009 Quantum communication using single photons from a semiconductor quantum dot emitting at a telecommunication wavelength. *J. Opt. A: Pure Appl. Opt.* **11** 054005
[15] Collins R J *et al* 2010 Quantum key distribution system in standard telecommunications fiber using a short wavelength single photon source *J. Appl. Phys.* **107** 073102

[16] Takemoto K, Nambu Y, Miyazawa T, Wakui K, Hirose S, Usuki T, Takatsu M, Yokoyama N, Yoshino K, Tomita A *et al* 2010 Transmission experiment of quantum keys over 50 km using high-performance quantum-dot single-photon source at 1.5 μm wavelength *Appl. Phys. Express* **3** 2802

[17] Heindel T *et al* 2012 Quantum key distribution using quantum dot single-photon emitting diodes in the red and near infrared spectral range *New J. Phys.* **14** 083001

[18] Heindel T, Schneider C, Lermer M, Kwon S H, Braun T, Reitzenstein S, Höfling S, Kamp M and Forchel A 2010 Electrically driven quantum dot-micropillar single photon source with 34% overall efficiency *Appl. Phys. Lett.* **96** 011107

[19] Reitzenstein S, Hofmann C, Gorbunov A, Strauß M, Kwon S H, Schneider C, Löffler A, Höfling S, Kamp M and Forchel M 2007 AlAs/GaAs micropillar cavities with quality factors exceeding 150.000 *Appl. Phys. Lett.* **90** 251109

[20] Weier H, Schmitt-Manderbach T, Regner N, Kurtsiefer C and Weinfurter H 2006 Free space quantum key distribution: Towards a real life application *Fortschr. Phys.* **54** 840

[21] Baumann V, Stumpf F, Schneider C, Kremling S, Worschech L, Forchel A, Höfling S and Kamp M 2012 Site-controlled InP/GaInP quantum dots emitting single photons in the red spectral range *Appl. Phys. Lett.* **100** 091109

[22] Schneider C, Heindel T, Huggenberger A, Niederstrasser T A, Reitzenstein S, Forchel A, Höfling S and Kamp M 2012 Microcavity enhanced single photon emission from an electrically driven site-controlled quantum dot *Appl. Phys. Lett.* **100** 091108

[23] Unrau W, Quandt D, Schulze J H, Heindel T, Germann T D, Hitzemann O, Strittmatter A, Reitzenstein S, Pohl U W and Bimberg D 2012 Electrically driven single photon source based on a site-controlled quantum dot with self-aligned current injection *Appl. Phys. Lett.* **101** 211119

[24] Deshpande S, Heo J, Das A and Bhattacharya P 2013 Electrically driven polarized single-photon emission from an InGaN quantum dot in a GaN nanowire *Nat. Commun.* **4** 1675

[25] Braun T, Unsleber S, Baumann V, Gschrey M, Rodt S, Reitzenstein S, Schneider C, Höfling S and Kamp M 2013 Cascaded emission of linearly polarized single photons from positioned InP/GaInP quantum dots *Appl. Phys. Lett.* **103** 191113